ADVANCED MATERIALS

DOI: 10.1002/adma.200601694

Anti-Lotus Effect for Nanostructuring at the Leidenfrost Temperature**

By *Mady Elbahri*, *Dadhichi Paretkar*, *Khaled Hirmas*, *Seid Jebril*, and *Rainer Adelung**

Nanoscale self-assembly is a concept that Nature has been making use of since the beginning of life,[1] and we have only recently started realizing its potential for achieving better control over materials properties. An overwhelming number of self-assembly fabrication methods for the formation of nanocluster arrangements on surfaces have been found, and they feature processes having various timescales, complexities, and versatilities. The fabrication of such structures can be discussed in terms of two processing steps that are independent of the actual process sequence. First, nanocomponents must be formed, which can be accomplished in various ways from precursors in the liquid, solid, or gas phases employing either chemical or physical deposition processes. In the second step, the challenge is to organize the segregated and deposited nanoparticles into structures or patterns on surfaces. Several approaches that use either a serial-writing-type process[2] or templates that allow fast parallel processing[3,4] have been formulated. More simple are the template-free approaches based on self-organization, which is the autonomous organization of components into patterns without human intervention.[5] Among all of these approaches, wet-chemical strategies utilizing fluid mechanics appear to be the simplest and most effective. Evaporation of drops on nonfunctionalized substrates has been used for the patterned deposition of solutes in DNA microarrays.[6] Furthermore, the ring deposition of particles from colloidal dispersions deposited as droplets has also been shown.[7] In addition to droplet drying, combined flow drying has been utilized for the deposition of semiconductor nanowires and nanotubes onto functionalized substrates.[8] The self-organization of matter into regular sub-micrometer- and nanoscale lines by using the wetting instability of a Langmuir–Blodgett film[9,10] as a cost-effective method has also been discussed. However, structuring of nanocluster arrays or wirelike morphologies from a droplet still faces certain challenges. Yawahare et al.[11] have demonstrated the room-temperature formation of lines from a drop if three prerequisites are met: evaporation between partially wetted surfaces, the presence of a pinning point, and the availability of a surfactant.

In contrast to the above approaches, this paper presents a droplet-deposition-based, template-free, and rapid (only a few seconds) approach for fabricating nanostructures without the use of any surfactant. Our general setup can be understood as the so-called "anti-Lotus effect". The Lotus effect[12] is well known for its removal of dust particles from the surface of a lotus leaf by gathering them into a droplet that is moving over the surface, thus cleaning it. The effect is based on the ability of certain surfaces to form spherical droplets with contact angles near 180° (i.e., superhydrophobic), enabling the incorporation of surface particles as well as a reduction in friction. In contrast to this, our work makes use of an anti-Lotus effect, in which the droplet *delivers* material while moving over the surface. In this case, a reduction in friction is achieved by employing the Leidenfrost effect, thus enabling the use of normal surfaces, such as plain silicon, as substrates.

If a liquid drop touches a hot solid having temperatures higher than the boiling point of the liquid, the lower part of the droplet will immediately evaporate and protect the rest of the droplet from further evaporating for a limited period of time. At this point, the drop is no longer in contact with the solid but levitates above its own vapor. Such a floating drop is called a Leidenfrost drop, after the German physicist who first reported the phenomenon some 250 years ago;[13] it is only recently that the scientific potential of this phenomenon has been realized.[14]

However, it must be noted that a random deposition of a solution drop is totally ineffective in fathering any technologically useful nanoscale structures, such as arrangements of well-separated patterns prepared from monodisperse particles, which often demand a high degree of organization. In order to deposit material from a droplet in an organized manner, a deeper insight into the underlying mechanism of the fluid drop is necessary. A drop drying slowly on a polar surface will typically lead to ring-shaped depositions at room temperature[7] rather than the thin films obtained at the Leidenfrost temperature, where the film homogeneity depends on the drop radius.[15,16]

To develop patterns at the Leidenfrost temperature, we made use of the reduced friction of the Leidenfrost droplet. This strategy is illustrated by the schematic in Figure 1. An

[*] Dr. R. Adelung, M. Elbahri, D. Paretkar, K. Hirmas, S. Jebril
Lehrstuhl für Materialverbunde
Technische Fakultät der Universität Kiel
Kaiserstrasse 2, 24143 Kiel (Germany)
E-mail: ra@tf.uni-kiel.de

[**] We thank Prof. F. Faupel for valuable support at all stages of this work and D. Lukas, K. Rätzke, and V. Zaporojtchenko for helpful discussions. Technical support from S. Rehders and R. Kloth is gratefully acknowledged. Furthermore, the authors thank the DFG for enabling the project by financial support in the Focus Program 1165 project AD183/4-2. Supporting Information is available online from Wiley InterScience or from the author.

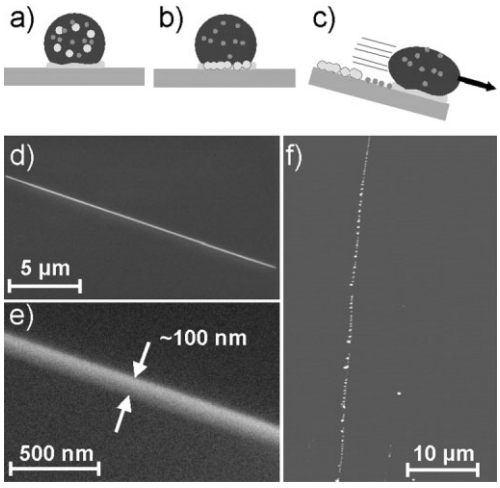

Figure 1. Line deposition of nanoparticles. a) Schematic of a droplet loaded with particles levitating on its own vapor at the Leidenfrost temperature. b) Selective deposition from a Leidenfrost droplet. c) Illustration of the motion of a droplet when the substrate is tilted, creating the anti-Lotus effect. Particles are delivered in lines from the droplet. d) Part of a nanowire composed of densely packed nanoparticles formed as depicted in the schematics in (a–c). e) Magnification of the image in (d). f) Depending on the concentration, chains of silver clusters can be found.

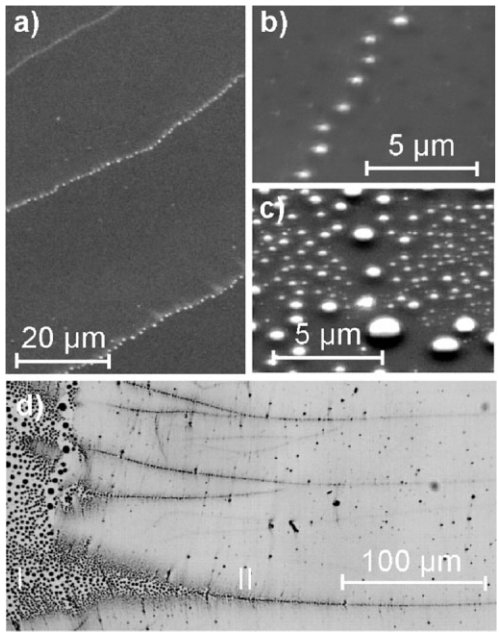

Figure 2. Particle size-selection during the deposition of ZnO particles from a suspension at the Leidenfrost temperature. a) Scanning electron microscopy (SEM) image of chains of ZnO particles with a quasi-similar size created by a running droplet. b) Magnification of a portion of the chain in (a). c) SEM image illustrating that before tilting the droplet, an area is created where grains of different sizes condense. d) Optical microscopy image showing the transition between the area and the line (I is the area before the droplet moves and II is the line of clusters).

extremely dilute solution of the desired material powder was prepared in water. A droplet from this solution was gently placed on a substrate, such as a silicon wafer, that was maintained at a temperature of 230 °C, which is the estimated Leidenfrost temperature for any suspension droplet. The drop was subsequently allowed to stay on the hot substrate for ca. 5 s before the substrate was tilted ca. 30° to the horizontal to exploit gravity for the propagation of the loaded droplet across the substrate surface (Fig. 1b and c). When a water droplet loaded with silver nanoparticles was subjected to the above procedure, wires (Fig. 1d and e) or cluster chains (Fig. 1f) were successfully produced.

The process works even when suspensions are prepared by using bulk powders. Conventional powders typically contain all types of grain sizes, including sub-micrometer- and nanometer-sized particles. For our experiments, a droplet was loaded with commercially available bulk zinc oxide powder. The resulting nanocluster chains are shown in Figure 2a and b. In this case, upon droplet deposition and just before tilting, the particles separated on the basis of their sizes. Typically, the largest particles left the droplet immediately, as shown in Figure 2c, followed by the comparatively smaller particles, as illustrated in Figure 1b and c. Apparently, the deposited area provided several self-pinning points for the droplet, from where the cluster lines start to stretch. Thus, upon tilting the substrate ca. 30°, several cluster chains parallel to the flow direction were deposited on the substrate simultaneously, as seen from the optical microscopy image in Figure 2d. Area I shows a comparatively larger range of cluster sizes representing the self-pinning area. Some of these will act as a center point for the line-stretching observed in area II, which has a significantly smaller cluster size range. Energy dispersive X-ray (EDX) line scans across the cluster chains reveal that nearly all of the material is concentrated along the lines.

Furthermore, such nanoparticle–cluster chains and wires can be fabricated by employing the overheated-temperature, nonequilibrium zone readily available underneath the droplet as a chemical reactor to produce nanoparticles directly from solution. A variety of chemicals, including silver nitrate and zinc acetate, were successfully subjected to a hot nonequilibrium vapor/liquid interface reaction for the creation of nanoparticles having a different chemical composition from their parent solution. Silver wires or nanocluster chains were obtained by reacting a solution of $AgNO_3$ at 180 °C, and ZnO was produced by the thermal decomposition of zinc acetate at 280 °C (the temperature of the bulk reaction).[17]

The anti-Lotus method was applied to a dilute silver nitrate solution, affording chains of silver clusters (Fig. 3a). The Ag clusters were homogeneous with a diameter of approximately 150 nm and an interparticle distance of 200 nm. During the EDX characterization, a pure silver signal from the line scan was obtained (nitrogen and oxygen are present at the noise level). When subjected to the same anti-Lotus procedure, a droplet of zinc acetate yielded dense wires of ZnO nanoclusters, as seen in Figure 3b. These results are remarkable, as both reactions take place at a temperature of ca. 230 °C. The temperature of the droplet (< 100 °C) is far too low to explain the occurrence of these reactions. It appears that only a thin

ADVANCED MATERIALS

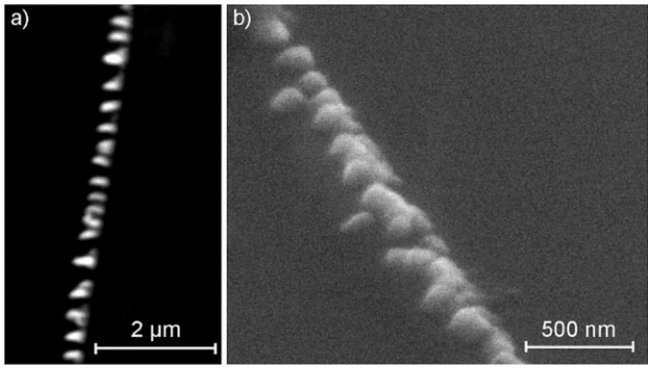

Figure 3. Scanning electron microscopy images of different particles generated by chemical decomposition. a) Silver and b) ZnO particles.

vapor phase region between the substrate and droplet can be considered as the reaction zone and provide sufficient temperatures (ca. 230 °C). Yet these reaction temperatures are still ca. 50 °C lower than the temperature required for forming bulk ZnO. Similar findings have recently been reported for the thermal-decomposition synthesis of ZnO nanorods.[18] The novel features of the anti-Lotus method, in addition to its ability to select and deposit particles in the nanoregime, offer the possibility for chemically transforming bulk material into nanoparticles and subsequently arranging them into ordered arrays with the help of a single, rapid step that lasts no more than 10–15 s.

The arrays obtained from the anti-Lotus depositions are a function of several parameters, such as droplet diameter, substrate temperature, and solution concentration. At the Leidenfrost temperature, a droplet with a radius above its capillary length (ca. 2.5 mm) forms a puddle flattened by gravity that will reduce the frictionless transport behavior observed for a comparatively smaller droplet. On the other hand, much larger droplets (ca. 50 mm) suffer from Rayleigh–Tylor instability.[16] From the above considerations and with the help of a series of experiments, we determined that a droplet diameter of ca. 10 mm yielded optimal results.

Additionally, it is noted that the floating behavior of the droplet can also be initiated at temperatures above the nucleate boiling point of the liquid, in which case the droplet lifetime tends to gradually increase. However the Leidenfrost temperature is defined as the local maximum in the evaporation lifetime of the droplet, and such a local maximum is assisted by the poor heat transfer between the substrate and the droplet, primarily because of the vapor encapsulating the droplet. If the vapor limiting the heat transfer happens to be loaded with salt, the salt may either increase or decrease the coefficient of heat transfer,[19] thus eventually dictating the droplet evaporation lifetime. For example, droplets containing ZnO salt in extremely low concentrations showed lifetimes near 14–16 s at the Leidenfrost temperature, which are approximately four times shorter than those of salt-free water droplets (ca. 73 s), yet long enough for our experimental procedure to go to completion. The decrease in the lifetime observed for the salt-loaded droplet could be attributed to the increase in the heat transfer within the droplet facilitated by the particles deposited during the early stages.

Apart from straight, parallel lines in series, nanoparticles can also be arranged in concentric circles with our Leidenfrost structuring. This patterning is attributed to a different and interesting phenomenon that also occurs at the Leidenfrost temperature, under slightly modified fluid dynamics, where droplet impact is emphasized. Interfacial, viscous, and capillary forces are the three basic forces governing the behavior of a droplet on a surface. At temperatures below the Leidenfrost temperature, a spreading behavior that results in the formation of a disklike thin film is observed upon impact.[20] However, this behavior changes if the process occurs at the Leidenfrost temperature, where a drop explosion takes place, as discussed previously.[21] Smaller droplets are formed upon impact due to the disintegration of the larger ones, which appears to be the source of the concentric rings in the present study. As the behavior of the droplet upon impact involves accounting for the complex interaction between several parameters,[22] for our preliminary experiments we have restricted ourselves to optimizing the working conditions for utilizing the impact technique as a new type of nanostructuring method.

Figure 4a shows the results of an impact from a drop loaded with zinc acetate. Rings consisting of ZnO nanorods are observed in the scanning electron microscopy (SEM) image. This process covers large areas with nanostructures more rapidly than in the case of line deposition because it can easily be performed in parallel with many droplets; therefore, within the same time frame, we can cover areas of any arbitrary size with the nanostructures. Figure 4b and c show that the resulting wires are composed of a dense assembly of rods. The well-known hexagonal structure for ZnO rods with a typical *z*-orientation can be clearly seen from these images and were also verified by EDX and X-ray photoelectron spectroscopy (XPS) measurements.

Dissipative structures[23] are known to be the driving force for self-organization and patterning in a system far from equilibrium. For nonequilibrium systems such as the anti-Lotus system, this effect could be attributed to the convective flow induced by the presence of a gradient effect known as a Marangoni instability. The precondition for this effect is the existence of heat or mass transfer in the system. In our case we have both a temperature gradient between the droplet and the hot surface and a concentration gradient created by the chemical reaction at the vapor/droplet interface. Whenever droplet dimensions are in the range of ca. 10 μm, as in the present case, thermocapillary-driven forces help separate the discrete smaller droplets from the original larger droplet and propel them rapidly through space. The combined effect of droplet splitting and droplet instability appears to be central to the formation of various complex and intersecting ring nanostructures.

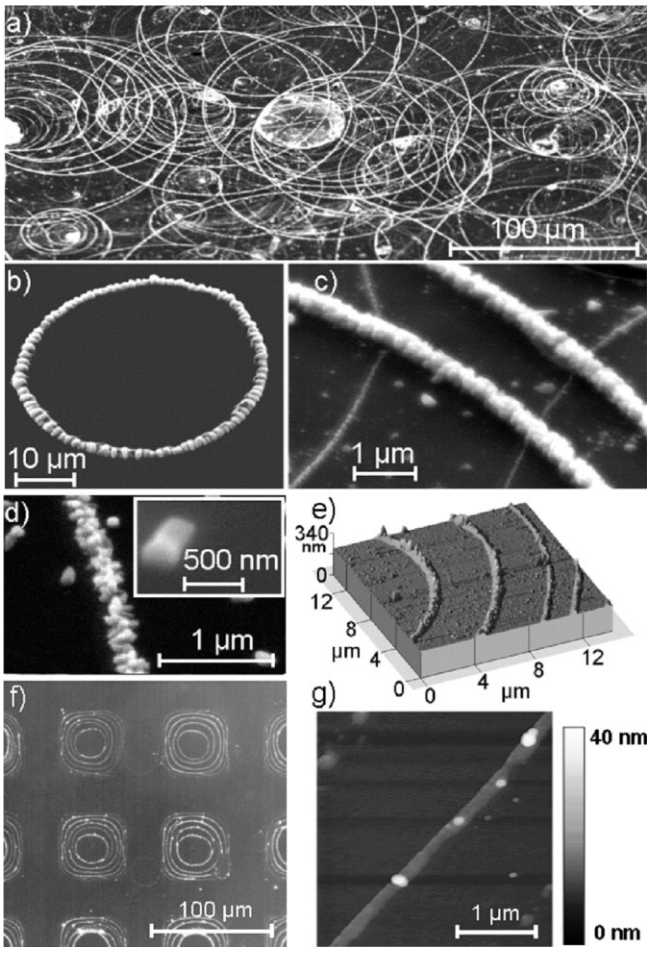

Figure 4. Microscopy images of rings of ZnO and silver nanoparticles formed by droplet disintegration at the Leidenfrost temperature. a) Overview showing intersecting ZnO circles; b) individual ZnO rings; and c) rings of different sizes intersecting each other. d) A magnified view of part of a ring revealing the hexagonal crystalline character. e) A 3D representation of an atomic force microscopy (AFM) image showing a part of a concentric silver-ring system that is aligned with help of a transmission electron microscopy grid. f) Dark-field optical microscopy image giving an overview of the reproducibility of the aligned ring systems. g) AFM image of a Ag ring with nanoscale diameters.

The structures discussed above have various applications. The silver chains have a particle-diameter-to-gap ratio of less than 1.5, which makes them suitable for the waveguide channel often used in optoelectronics[24] as well as nonlinear optical applications.[25] The ZnO nanowires obtained appear to consist of an agglomerate of nanorods, indicating a potentially larger surface-area-to-volume ratio than the one usually observed in the case of single-crystalline materials. As a high surface-area-to-volume ratio at the nanoscale is beneficial for sensing extremely small biological and chemical species,[26] we hope that the ZnO rod agglomerates obtained by using our extremely inexpensive approach can replace those grown by conventional means. Furthermore, at the contact points of the individual rods there exist so-called chemically responsive interparticle boundaries (CRIBs),[26] which are known to enhance sensory properties. The capability of such devices is presently undergoing investigation in our laboratory.

To take a fabrication process beyond the small scale of the laboratory, it is important to be able to achieve exact placement of the nanostructures on a substrate. Similar to the diffusion process,[11] alignment of the structures in the present case is possible by combining our approach with a top-down strategy. A micropatterned grid with square-type holes 50 µm by 50 µm, similar to those often used for transmission electron microscopy (TEM) sample preparation, was employed to predefine the arrangement of the structure. By simply placing the TEM grid onto the silicon substrate during the process of droplet deposition, the large droplet became divided equally into smaller droplets, each forming a 50 µm by 50 µm pool. Figure 4e shows a part of the concentric ring system that was formed at each pool site. The atomic force microscopy (AFM) image shows silver wires, which are obtained from silver nitrate as explained above. A low-magnification image (optical microscopy, dark field) in Figure 4f confirms the regularity of the pattern obtained without any further optimization. The image in Figure 4g reveals that the silver rings may be able to form nanoscale features, as in the case of ZnO.

In summary, we have demonstrated a chemical reaction directly onto a substrate that rapidly produces nanoparticles in one step while subsequently ordering them into arrays of parallel wires and rings. Furthermore, the anti-Lotus method at the Leidenfrost temperature is a new, environmentally friendly system for the direct production, deposition, and patterning of nanostructures on a surface. This 'all-in-one' template-free procedure could replace the multitude of competing complex processes presently in use. Furthermore, this approach is generic and could easily be modified for any desired chemicals with very few limitations. By combining this approach with simple top-down patterning strategies such as masks, the rapid large-scale fabrication of well-organized nanoscale morphologies appears realistic. Utilizing the nonequilibrium processes that occur in overheated droplets on surfaces might be a promising way to accomplish chemical reactions in a different manner, as in the case of ZnO.

Experimental

All samples were fabricated on a silicon substrate, which was cleaned with isopropyl alcohol in an ultrasonic bath and dried in air before use. For the fabrication of silver nanowires (Fig. 1), a water droplet was loaded with a dispersed silver nanopowder, (100 nm, weight ratio 1:150), 99.95 %, from Sigma–Aldrich, Schnelldorf, Germany. In the case of zinc oxide nanoclusters (Fig. 2), a water droplet was loaded with a dispersed zinc oxide powder (weight ratio 1:50), 99.99 %, Sigma–Aldrich, Schnelldorf, Germany. The silver nanoclusters in Figures 3a and 4e–g were generated from a droplet of a 10^{-3} M and a 3×10^{-5} M solution of silver nitrate, 99.99995 %, Alfa Aesar, Karlsruhe, Germany. Zinc oxide rings and wires (Fig. 4a–d) were generated from a droplet of a 10^{-3} M solution of zinc acetate, 99.99 %, Sigma–Aldrich, Schnelldorf, Germany. The impact distance was typically 10–15 cm. For imaging and analysis, a Phillips XL 30 scanning electron microscope equipped with an EDAX EDX detector was utilized

ADVANCED MATERIALS

to analyze the surface geometry and the chemical composition. AFM images were obtained with a Park Autoprobe instrument.

Received: July 26, 2006
Revised: January 16, 2007
Published online: April 13, 2007

[1] C. P. Poole, Jr., F. J. Owens, *Introduction to Nanotechnology*, Wiley-VCH, Weinheim, Germany **2003**.
[2] Y. Xia, P. Yang, Y. Sun, Y. Wu, B. Mayers, B. Gates, Y. Yin, F. Kim, H. Yan, *Adv. Mater.* **2003**, *15*, 353.
[3] R. Adelung, O. C. Aktas, J. Franc, A. Biswas, R. Kunz, M. Elbahri, J. Kanzow, U. Schürmann, F. Faupel, *Nat. Mater.* **2004**, *3*, 375.
[4] M. Elbahri, S. K. Rudra, S. Wille, S. Jebril, M. Scharnberg, D. Paretkar, R. Kunz, H. Rui, A. Biswas, R. Adelung, *Adv. Mater.* **2006**, *18*, 1059.
[5] G. M. Whitesides, B. Grzybowski, *Science* **2002**, *295*, 630.
[6] T. Heim, S. Preuss, B. Gerstmayer, A. Bosio, R. Blossey, *J. Phys.: Condens. Matter* **2005**, *17*, 703.
[7] R. D. Deegan, O. Bakajin, T. F. Dupont, G. Huber, S. R. Nagel, T. A. Witten, *Nature* **1997**, *389*, 827.
[8] Y. Huang, X. Duan, Q. Wei, C. M. Lieber, *Science* **2001**, *291*, 630.
[9] M. Gleiche, L. F. Chi, H. Fuchs, *Nature* **2000**, *403*, 6766.
[10] X. Chen, M. Hirtz, H. Fuchs, L. Chi, *Adv.Mater.* **2005**, *17*, 2881.
[11] S. Yawahare, K. M. Craig, A. Scherer, *Nano Lett.* **2006**, *6*, 271.
[12] W. Barthlott, C. Neinhuis, *Planta* **1997**, *202*, 1.
[13] J. G. Leidenfrost, *De Aquae Communis Nonnullis Qualitatibus Tractatus*, Johann Straube, Duisburg, Germany **1756**.
[14] D. Quere , A. Ajdar, *Nat. Mater.* **2006**, *5*, 429.
[15] N. Tsapis, E. R. Dufresne, S. S. Sinha, C. S. Riera, J. W. Hutchinson, L. Mahadevan, D. A. Weitz, *Phys. Rev. Lett.* **2005**, *94*, 018 302.
[16] A.-L. Biance, C. Clanet, D. Quere, *Phys. Fluids* **2003**, *15*, 1632.
[17] A. V. Ghule, K. Ghule, C. Y. Chen, W. Y. Chen, S. H. Tzing, H. Chang, Y. C. Ling, *J. Mass Spectrom.* **2004**, *39*, 1202.
[18] X. Su, Z. Zhang, Y. Wang, M. Zhu, *J. Phys. D: Appl. Phys.* **2005**, *38*, 3934.
[19] M. D. King, J. C. Yang, W. S. Chien, W. L. Grosshandler, in *Proc. ASME National Heat Transfer Conference* (Eds: G S. Dulikravich, K. A. Woodbury), The American Society of Mechanical Engineers, New York **1997**.
[20] M. Rein *Fluid. Dyn. Res.* **1993**, *12*, 61.
[21] J. D. Bernardin, I. Mudawar, *Trans ASME* **1999**, *121*, 894.
[22] S. L. Manzello, J. C. Yang, *Proc. R. Soc. London A* **2002**, *458*, 2417.
[23] G. Nicolis, J. F. G. Auchmuty, *Proc. Natl. Acad. Sci. USA* **1974**, *71*, 2748.
[24] S. A. Maier, P. G. Kik, H A. Atwater, S. Meltzer, E. Harel, B. E. Koel, A. A. G. Requicha, *Nat. Mater.* **2003**, *2*, 229.
[25] M. S. Hu, H. L. Chen, C. H. Shen, L. S. Hong, B. R. Huang, K. H. Chen, L. C. Chen, *Nat. Mater.* **2006**, *5*, 102.
[26] B. J. Murray, E. C. Walter, R. M. Penner, *Nano Lett.* **2004**, *4*, 665.

